Journal of Sound and Vibration (1999) **220**(4), 641–657
Article No. jsvi.1998.1960, available online at http://www.idealibrary.com on IDEAL

FORCED ASYMMETRIC RESPONSE OF LINEARLY TAPERED CIRCULAR PLATES

A. P. Gupta

Department of Mathematics, University of Roorkee, Roorkee 247667 (*U.P.*), *India*

AND

N. Goyal

Department of Mathematics, Birla Institute of Technology and Science, Pilani 333031 (*Rajasthan*), *India*

(*Received* 30 *July* 1996, *and in final form* 19 *August* 1998)

The eigenfunction method is used to analyze the asymmetric response of linearly tapered circular plates subjected to transverse loads, uniformly distributed over an annular sectorial area of the plate. The analysis is based on the classical plate theory. Numerical results are presented graphically for the transverse deflection and stresses of the plate for various combinations of plate and loading parameters. Results obtained, as a particular case, for a plate of constant thickness subjected to an off-center half-sine pulse point load are compared with previously published results and found to match exactly.

1. INTRODUCTION

Circular plates of variable thickness are widely used in several engineering fields. In particular, the title problem is related to the loading condition in machine parts such as diaphragms of turbines.

Although the free vibration problem of circular and annular plates of variable thickness with various complicating effects has been taken up by many researchers [1–4], very little work is available on the forced motion of circular plates of variable thickness and even that is limited to their axisymmetric response only, namely, Laura *et al*. [5], Irie *et al*. [6], Greco and Laura [7], and Gupta and Goyal [8, 9]. The authors have so far not come across any paper dealing with the asymmetric forced response problem of circular plates of variable thickness.

Several research papers dealing with the forced asymmetric response of circular plates of constant thickness can be found in the literature. Reismann [10] studied the forced vibration of a clamped circular plate subjected to an arbitrarily placed, harmonically oscillating, transverse, concentrated force, utilizing the concept of singularity solutions. Mcleod and Bishop [11] presented solutions for a variety of special cases of forced vibration of circular plates with simply-supported, free, clamped, and sliding boundary conditions. Anderson [12] presented a finite integral transform method to study the forced response of circular plates.

0022–460X/99/090641 + 17 $30.00/0

Ramakrishnan and Kunukkasseril [13] have analytically analyzed the response of circular plates to asymmetric loadings. Kunukkasseril and Ramakrishnan [14] analyzed the effects of sonic boom on circular bridge panels. Kunukkasseril and Chandrasekaran [15] studied the impact of concentrated loading on circular plates, experimentally. Fisher [16] presented a modal analysis solution for the transient asymmetric response problem of thin circular plates. Yang [17] proposed a generalized Kelvin-function solution for a class of vibrating circular plate problems. He applied it to study the forced vibration of the injector plate due to pressure oscillation in the combustion chamber of a liquid rocket engine and the circular lid of an underwater container subjected to water motion.

In the present paper, forced asymmetric response of linearly tapered circular plates is analyzed by the eigenfunction method. The exact free vibration frequencies and mode shapes are obtained by the Frobenius method, which enables us to solve the integrals involved in the orthogonality condition of mode shapes easily. A more detailed account of the advantages of the method can be found in the authors' earlier papers [8, 9]. A clamped plate subjected to a half-sine pulse load, distributed uniformly over an annular sectorial area of the plate is considered as an example problem. Numerical results are presented graphically for the transverse deflection and stresses of the plate for various combinations of plate and loading parameters. Results obtained, as a particular case, for a plate of constant thickness subjected to an off-center half-sine pulse point load are compared with previously published results and found to match exactly.

2. EQUATION OF MOTION

The equation of motion governing the forced asymmetric response of a linearly tapered circular plate (see Figure 1(a)) according to classical plate theory is taken as

$$D\nabla^4 w + D_{,r}\left[2w_{,rrr} + \frac{2+\nu}{r}w_{,rr} - \frac{1}{r^2}w_{,r} + \frac{2}{r^2}w_{,r\theta\theta} - \frac{3}{r^3}w_{,\theta\theta}\right] + D_{,rr}\left[w_{,rr} + \frac{\nu}{r}w_{,r} + \frac{\nu}{r^2}w_{,\theta\theta}\right] + \rho h w_{,tt} = f(r,\theta,t) \quad (1)$$

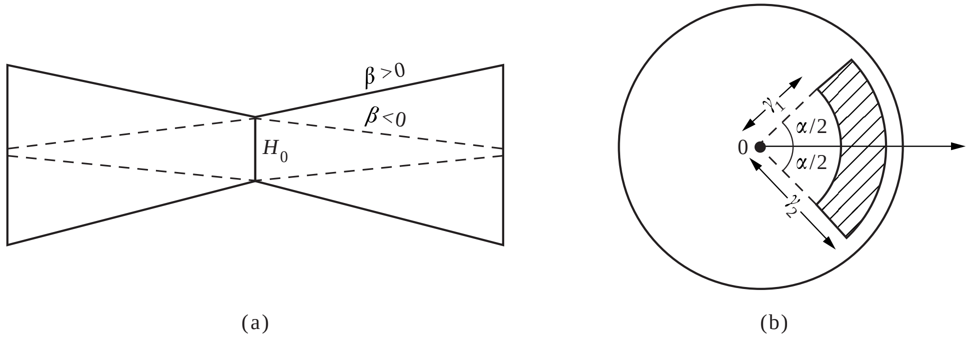

Figure 1. (a) Transverse section of plate and (b) loading configuration.

where

$$\nabla^4 = \left(\frac{\partial^2}{\partial r^2} + \frac{1}{r}\frac{\partial}{\partial r} + \frac{1}{r^2}\frac{\partial^2}{\partial \theta^2}\right)\left(\frac{\partial^2}{\partial r^2} + \frac{1}{r}\frac{\partial}{\partial r} + \frac{1}{r^2}\frac{\partial^2}{\partial \theta^2}\right)$$

is the polar biharmonic operator, $D = Eh^3/12(1-v^2)$ is the flexural rigidity of the plate, and $w, f, h_0, \beta, \rho, v$ and t are the transverse deflection, transverse force per unit area, thickness at the center, taper constant, density of the plate, Young's modulus, Poisson ratio, and time respectively.

The above equation is made non-dimensional to get

$$\begin{aligned}
&\frac{H^3}{R^4}[R^4 W_{,RRRR} + 2R^3 W_{,RRR} - R^2 W_{,RR} + RW_{,R} + 2R^2 W_{,RR\theta\theta} \\
&\quad - 2RW_{,R\theta\theta} + 4W_{,\theta\theta} + W_{,\theta\theta\theta\theta}] \\
&\quad + \frac{3H^2 H_{,R}}{R^3}[2R^3 W_{,RRR} + (2+v)R^2 W_{,RR} - RW_{,R} + 2RW_{,R\theta\theta} - 3W_{,\theta\theta}] \\
&\quad + \frac{3(2HH_{,R}^2 + H^2 H_{,RR})}{R^2}[R^2 W_{,RR} + vRW_{,R} + vW_{,\theta\theta}] + 12HW_{,TT} \\
&= 12F(R, \theta, T),
\end{aligned} \tag{2}$$

where

$$H = H_0(1+\beta R), \quad R = r/a, \quad H = h/a,$$

$$H_0 = h_0/a, \quad W = w/a, \quad F = 12(1-v^2)f/E, \quad T = t\sqrt{E/\{\rho a^2(1-v^2)\}},$$

The homogeneous boundary conditions are that one member of each of the following pairs vanish at the edge $R = 1$:

$$(W, V_R) \quad \text{and} \quad (W_{,R}, M_R), \tag{3}$$

where

$$V_R = M_{R,R} + \frac{M_R - M_\theta + 2M_{R\theta,\theta}}{R}, \qquad M_R = \frac{-H^3}{12}\left(W_{,RR} + \frac{v}{R}W_{,R} + \frac{v}{R^2}W_{,\theta\theta}\right),$$

$$M_\theta = \frac{-H^3}{12}\left(vW_{,RR} + \frac{W_{,R}}{R} + \frac{W_{,\theta\theta}}{R^2}\right) \quad \text{and} \quad M_{R\theta} = \frac{-H^3(1-v)}{12}\left(\frac{W_{,R\theta}}{R} - \frac{W_{,\theta}}{R^2}\right).$$

The initial conditions involves the specification of

$$W(R, \theta, 0) = W^0(R, \theta) \quad \text{and} \quad W_{,T}(R, \theta, 0) = W^0_{,T}(R, \theta). \tag{4}$$

3. METHOD OF SOLUTION

3.1. FREE VIBRATION ANALYSIS

For free vibration, the solution assumed as

$$W(R, \theta, T) = W_{jm}(R) \cos m\theta \, e^{i\Omega_{jm} T}, \tag{5}$$

where j $(=0, 1, 2, 3, \ldots)$ denotes the number of nodal circles, and m $(=0, 1, 2, \ldots)$ denotes the number of nodal diameters, is substituted in the homogeneous differential equation (2), obtained by setting $F = 0$. It gives

$$\begin{aligned}
&(1 + \beta R)^2 \left[W_{jm,RRRR} + \frac{2}{R} W_{jm,RRR} - \frac{1 + 2m^2}{R^2} W_{jm,RR} \right. \\
&\left. + \frac{1 + 2m^2}{R^3} W_{jm,R} + \frac{m^2(m^2 - 4)}{R^4} W_{jm} \right] \\
&+ 3\beta(1 + \beta R) \left[2W_{jm,RRR} + \frac{2 + \nu}{R} W_{jm,RR} - \frac{1}{R^2} W_{jm,R} \right. \\
&\left. - \frac{2m^2}{R^2} W_{jm,R} + \frac{3m^2}{R^3} W_{jm} \right] \\
&+ 6\beta^2 \left[W_{jm,RR} + \frac{\nu}{R} W_{jm,R} - \frac{m^2 \nu}{R^2} W_{jm} \right] - \omega_{jm}^2 W_{jm} = 0,
\end{aligned} \tag{6}$$

where $\omega_{jm}^2 = 12\Omega_{jm}^2 / H_0^2$.

The Frobenius method is used to solve the above equation. The solution is assumed as

$$W_{jm}(R) = \sum a_{jmk} R^{k + c}, \qquad a_{jm0} \neq 0, \tag{7}$$

where the summation over integer k is taken from 0 to ∞.

In the analysis to follow, the suffixes j and m of a_{jmk} are dropped for the sake of convenience. The solution (7) is substituted into equation (6). The indicial equation, obtained by equating to zero the coefficient of the lowest power of R has roots $c = -m$, $-m + 2$, m, and $m + 2$. The solutions corresponding to the indicial roots $-m$ and $-m + 2$ are singular at $R = 0$ and are therefore omitted. Equating to zero the coefficients of next higher power of R gives $a_1 = -3\beta(1 - \nu)m(m - 1)/(4m^2 - 1)$ and a_2 as indeterminate.

The recurrence relation is obtained as

$$
\begin{aligned}
a_k = -[\beta[(k+m-1)\{(k+m-2)\{2(k+m-1)^2 - 4 + 3v - 4m^2\}\\
-(1+2m^2)(k+m-1-m^2)]a_{k-1}\\
+\beta^2[(k+m-2)(k+m-3)\{(k+m-2)(k+m+1) + 1 + 3v - 2m^2\}\\
+ 2(k+m-2)(3v-1-2m^2)\\
+ (5-6v)m^2 + m^4]a_{k-2} - \omega_{jm}^2 a_{k-4}]/\{k(k-2)(k+2m)(k+2m-2)\}, \quad (8)
\end{aligned}
$$

where $k = 3, 4, 5, \ldots$, a_0 and a_2 are the arbitrary constants and $a_{-1} = 0$.

In terms of the arbitrary constants, the above recurrence relation can be written as

$$a_k = a_0 f_k^0 + a_2 f_k^2,$$

where

$$
\begin{aligned}
f_k^p = -[\beta[(k+m-1)\{(k+m-2)\{2(k+m-1)^2 - 4 + 3v - 4m^2\}\\
-(1+2m^2)(k+m-1-m^2)] f_{k-1}^p\\
+\beta^2[(k+m-2)(k+m-3)\{(k+m-2)(k+m+1) + 1 + 3v - 2m^2\}\\
+2(k+m-2)(3v-1-2m^2)\\
+(5-6v)m^2 + m^4] f_{k-2}^p - \omega_{jm}^2 f_{k-4}^p]/\{k(k-2)(k+2m)(k+2m-2)\},
\end{aligned}
$$

$p = 0$ and 2, $k = 3, 4, 5, \ldots$, and $f_0^0 = 1$, $f_1^0 = -3\beta(1-v)m(m-1)/(4m^2-1)$, $f_2^0 = 0$, $f_0^2 = 0$, $f_1^2 = 0$, $f_2^2 = 1$, and $f_{-1}^p = 0$.

The free vibration solution (7) therefore takes the form

$$W_{jm}(R) = \sum (a_0 f_k^0 + a_2 f_k^2) R^{k+m}. \quad (9)$$

3.2. CONVERGENCE OF SOLUTION

To test the convergence of solution (9), the recurrence relation (8) is divided by a_{k-4} and the limit is taken as $k \to \infty$. This gives

$$P^4 + 2\beta P^3 + \beta^2 P^2 = 0,$$

where

$$P^n = \lim_{k\to\infty} \left(\frac{a_k}{a_{k-n}}\right).$$

The roots of the above equation are $P = 0, 0, -\beta$, and $-\beta$, suggesting that the solution is uniformly convergent in the interval [0, 1] for $|\beta| < 1$.

3.3. ORTHONORMALITY CONDITION

The orthonormality condition of the normal modes of vibration is obtained as

$$\int_0^1 HW_{jm}W_{km}R\,\mathrm{d}R=\delta_{jk}, \tag{10}$$

where δ_{jk} is the Krönecker delta.

3.4. FORCED MOTION ANALYSIS

A solution to the forced motion problem posed by equation (2), the boundary conditions (3), and the initial conditions (4), is assumed in the form

$$W(R,\theta,T)=\sum\sum W_{jm}(R)\cos m\theta g_{jm}(T), \tag{11}$$

where W_{jm} are the mode shape functions given by equation (9). The summations over j and m are taken from 0 to ∞. The substitution of this solution in equation (2) gives

$$\begin{aligned}\sum\sum\Bigg[\Bigg(&\frac{H^3}{R^4}\{R^4W_{jm,RRRR}+2R^3W_{jm,RRR}-R^2W_{jm,RR}+RW_{jm,R}-2m^2R^2W_{,jm,RR}\\&+2m^2RW_{jm,R}-4m^2W_{jm}-m^4W_{jm}\}+\frac{3H^2H_{,R}}{R^3}\{2R^3W_{jm,RRR}\\&+(2+v)R^2W_{jm,RR}-RW_{jm,R}-2m^2RW_{jm,R}+3m^2W_{jm}\}\\&+\frac{6HH_{,R}^2}{R^2}\{R^2W_{jm,RR}+vRW_{jm,R}+m^2vW_{jm}\}\Bigg)g_{jm}+12HW_{jm}g_{jm,TT}\Bigg]=12F.\end{aligned}$$

Now, the use of equation (6), governing the free vibration in the jmth mode, leads to

$$\sum_j H[g_{jm,TT}+\Omega_{jm}^2g_{jm}]W_{jm}=F_m(R,T),\qquad m=0,1,2,\ldots,$$

where

$$F_0(R,T)=\frac{1}{\pi}\int_0^{\pi}F(R,\theta,T)\,\mathrm{d}\theta,$$

and

$$F_m(R, T) = \frac{2}{\pi}\int_0^{\pi} F(R, \theta, T)\cos m\theta \, \mathrm{d}\theta, \qquad m = 1, 2, 3, \ldots .$$

Multiplying the above equation by W_{km}, integrating over the plate and using the orthogonality condition (10), one gets

$$g_{jm,TT} + \Omega_{jm}^2 g_{jm} = G_{jm}(T), \tag{12}$$

where

$$G_{jm}(T) = \int_0^1 W_{jm}(R)F_m(R, T)R \, \mathrm{d}R, \qquad m = 0, 1, 2, \ldots . \tag{13}$$

The solution of equation (12), obtained by using the Laplace transformation technique, is given by

$$\Omega_{jm}g_{jm}(T) = \Omega_{jm}g_{jm}(0)\cos\Omega_{jm}T + g_{jm,T}(0)\sin\Omega_{jm}T$$
$$+\int_0^1 G_{jm}(\tau)\sin\Omega_{jm}(T-\tau)\,\mathrm{d}\tau, \tag{14}$$

where $g_{jm}(0)$ and $g_{jm,T}(0)$ are the constants of integration to be determined from the initial conditions. Putting $T = 0$ in equation (11), one gets

$$W(R, \theta, 0) = W^0(R, \theta) = \sum\sum W_{jm}(R)\cos m\theta g_{jm}(0),$$

and

$$W_{,T}(R, \theta, 0) = W^0_{,T}(R, \theta) = \sum\sum W_{jm}(R)\cos m\theta g_{jm}(0).$$

Multiplying these relations by W_{km}, integrating over the plate and using the orthogonality condition (10), one gets

$$g_{jm}(0) = \int_0^1 HW_{jm}W^0R \, \mathrm{d}R \quad \text{and} \quad g_{jm,T}(0) = \int_0^1 HW_{jm}W^0_{,T}R \, \mathrm{d}R. \tag{15}$$

The radial and tangential stresses, at the top fiber are given by

$$\sigma_R = -\frac{H}{2}\sum\sum\left(W_{jm,RR} + \frac{\nu}{R}W_{jm,R} - \frac{m^2\nu}{R^2}W_{jm,R}\right)g_{jm}(T)\cos m\theta.$$

$$\sigma_\Theta = -\frac{H}{2}\sum\sum\left(\nu W_{jm,RR} + W_{jm,R} - \frac{m^2}{R^2}W_{jm,R}\right)g_{jm}(T)\cos m\theta. \tag{16}$$

This completes the formal solution of the forced asymmetric motion problem of a linearly tapered circular plate.

4. EXAMPLE PROBLEMS

4.1. BOUNDARY CONDITIONS AND FREQUENCY EQUATIONS

For a plate clamped at the boundary, one has $W = W_{,R} = 0$ at $R = 1$, which reduces to $W_{jm} = W_{jm,R} = 0$ at $R = 1$. These boundary conditions give

$$a_0 \sum f_k^0 + a_2 \sum f_k^2 = 0 \quad \text{and} \quad a_0 \sum (k+m) f_k^0 + a_0 \sum (k+m) f_k^2 = 0, \tag{17}$$

and therefore, the frequency equation is obtained as

$$\left(\sum f_k^0\right)\left(\sum (k+m) f_k^2\right) - \left(\sum f_k^2\right)\left(\sum (k+m) f_k^0\right) = 0. \tag{18}$$

The unique mode shape functions obtained by using the relations (17) and the mode normalization condition (10) are

$$W_{jm}(R) = a_0 \sum (f_k^0 - A f_k^2) R^{k+m}, \tag{19}$$

where

$$A = \left(\sum f_k^0\right) \Big/ \left(\sum f_k^2\right)$$

and

$$\frac{1}{a_0^2} = H_0 \sum \sum (f_k^0 f_l^0 - 2A f_k^0 f_l^2 + A^2 f_k^2 f_l^2)\left(\frac{1}{k+l+2m+2} + \frac{\beta}{k+l+2m+3}\right),$$

the summation over l also being taken from 0 to ∞.

4.2. INITIAL CONDITIONS

The initial displacement and initial velocity of the plate are assumed to be zero, that is $W^0(R, \theta) = W^0_{,T}(R, \theta) = 0$, so that from equation (15) one gets

$$g_{jm}(0) = g_{jm,T}(0) = 0. \tag{20}$$

4.3. LOADING CONDITION

The forced motion problem of the plate is analyzed for half-sine pulse, uniformly distributed load (see Figure 1(b) for loading configuration) given by

$$F(R, \theta, T) = \begin{cases} \dfrac{-2P_0}{\alpha(\gamma_2^2 - \gamma_1^2)} \sin(\pi T/t_1)[1 - U(T - t_1)], & \text{for } -\alpha/2 \leqslant \theta \leqslant \alpha/2 \text{ and } \gamma_1 \leqslant R \leqslant \gamma_2, \\ 0, & \text{elsewhere,} \end{cases} \tag{21}$$

where $U(T)$ represents the unit-step function.

The mode shape functions from equation (19) and the loading condition given by equation (21) are substituted into equation (13). $G_{jm}(T)$ thus obtained is substituted into equation (14) along with the initial conditions (20) to get

$$g_{jm} = \begin{cases} S_{jm}, & \text{for } m = 0 \\ 2S_{jm} \sin(m\alpha/2)/(m\alpha/2), & \text{for } m = 1, 2, 3, \ldots \end{cases} \quad T < t_1, \tag{22}$$

where

$$S_{jm} = \frac{P_0 t_1 [\Omega_{jm} \sin(\pi T/t_1) - \pi \sin(\Omega_{jm} T)]}{\pi \Omega_{jm} (\pi^2 - \Omega_{jm}^2 t_1^2)(\gamma_2^2 - \gamma_1^2)}$$

$$\times a_0 \sum (f_k^0 - A f_k^2) \left(\frac{\gamma_2^{k+m+2} - \gamma_1^{k+m+2}}{k+m+2} \right) \forall m.$$

$$g_{jm} = \begin{cases} S^*_{jm}, & \text{for } m = 0 \\ 2S^*_{jm} \sin(m\alpha/2)/(m\alpha/2), & \text{for } m = 1, 2, 3, \ldots \end{cases} \quad T \geqslant t_1, \tag{23}$$

where

$$S^*_{jm} = \frac{2P_0 \sin\{\Omega_{jm}(t_1/2 - T)\} \cos(\Omega_{jm} t_1/2)}{\Omega_{jm} (\pi^2 - \Omega_{jm}^2 t_1^2)(\gamma_2^2 - \gamma_1^2)}$$

$$\times a_0 \sum (f_k^0 - A f_k^2) \left(\frac{\gamma_2^{k+m+2} - \gamma_1^{k+m+2}}{k+m+2} \right) \forall m.$$

The transverse deflection and the radial stress for the forced motion problem are obtained by substituting $W_{jm}(R)$ from equation (19) and $g_{jm}(T)$ from equation (22)/(23), into expressions (11) and (16), respectively.

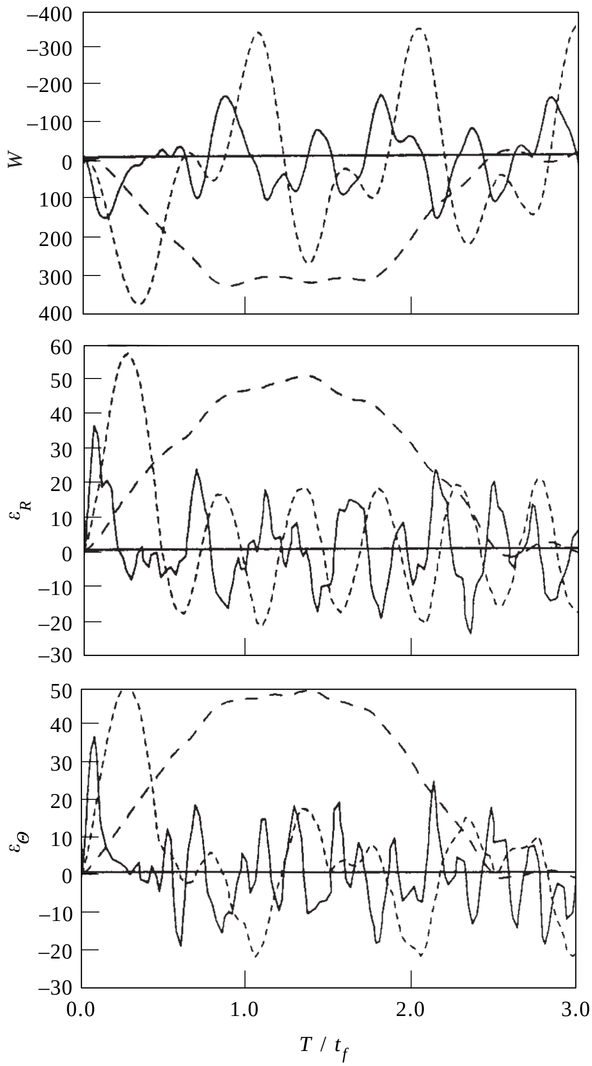

Figure 2. W, ε_R and ε_Θ under the load at $R = 0{\cdot}5$, $\theta = 0°$ for plates subjected to pulse load for various pulse durations. $H_0 = 0{\cdot}02$, $\beta = 0{\cdot}0$.; ——. $R_f = 0{\cdot}1$; – – –, 0·45; —— —, 2·5.

5. RESULTS AND DISCUSSION

The series involved in the characteristic equation (equation (18)) are summed up to an accuracy of 10^{-8}. The series occurring in the subsequent analysis are summed up to the same number of terms as taken in each earlier corresponding series. The roots of the characteristic equation are computed by the bisection method with a tolerance of 10^{-5}. A clamped plate subjected to constant and half-sine pulse loads is treated as an example problem. Numerical results are presented graphically for the transverse deflection (W/P_0), radial stress (σ_R/P_0) and tangential stress (σ_Θ/P_0). The series for transverse deflections and stresses (equations (11) and (16), respectively) are summed up to $j = 10$ and $m = 9$, which assures an accuracy of five decimal places.

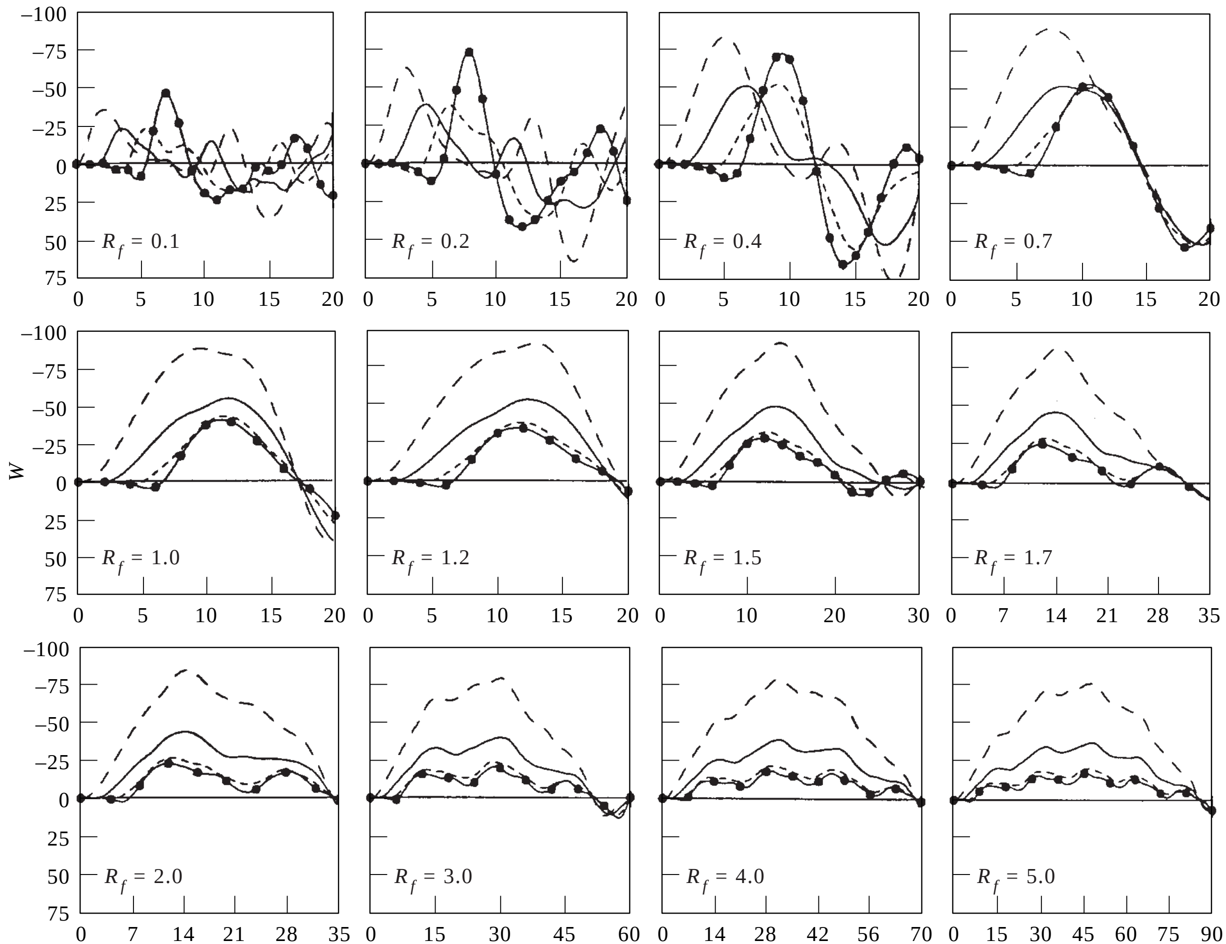

Figure 3. Effect of pulse duration on W at $R = 0{\cdot}5$. $H_0 = 0{\cdot}1$, $\beta = 0{\cdot}3$, $\alpha = 20^\circ$, $\gamma_1 = 0{\cdot}4$, $\gamma_2 = 0{\cdot}6$. — —, $\theta = 0^\circ$; ——, 60°; – – –, 120°; —●—, 180°.

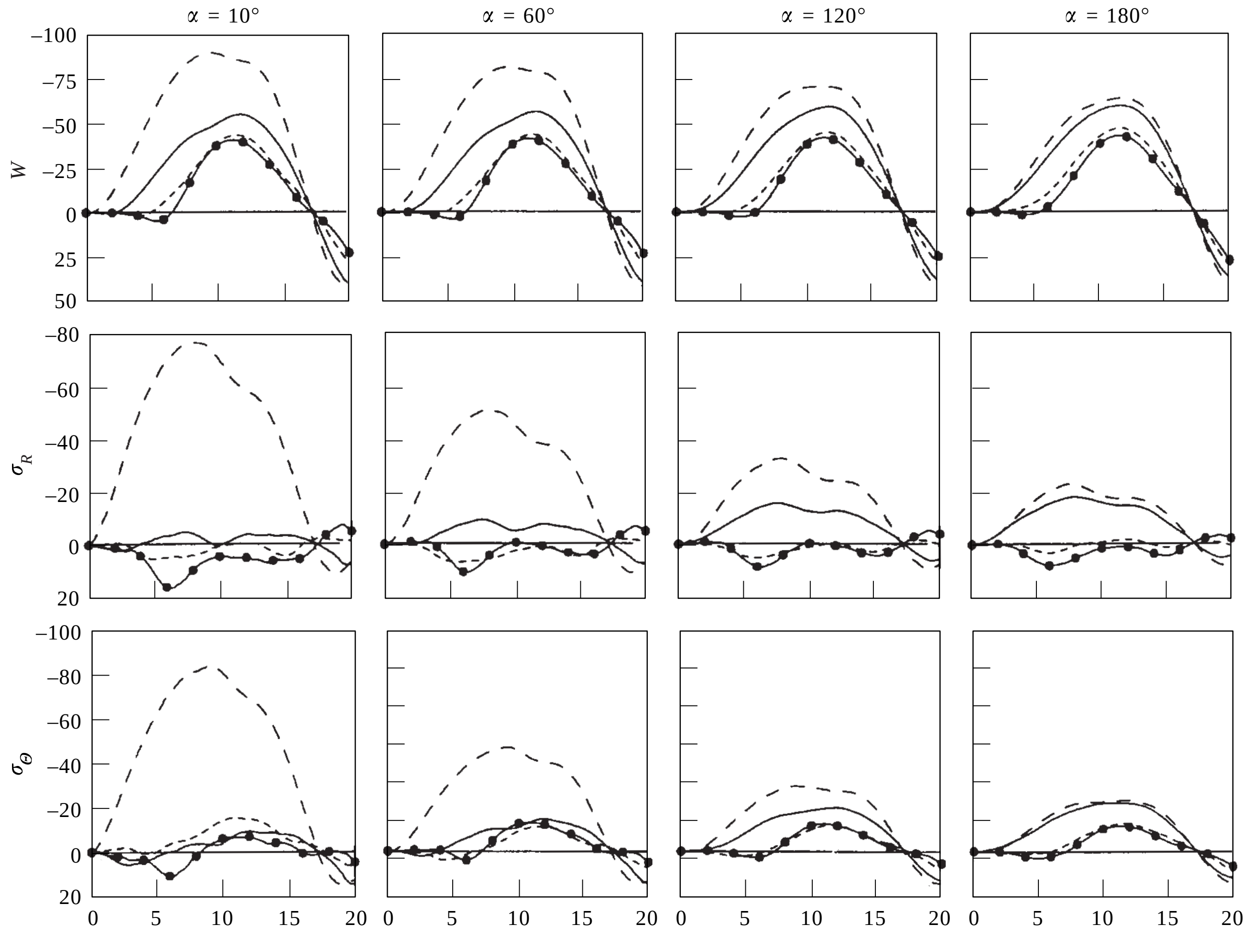

Figure 4. W, σ_R and σ_Θ at $R = 0{\cdot}5$ for plates subjected to pulse load for increasing angular span of load. $H_0 = 0{\cdot}01$, $\beta = 0{\cdot}3$, $R_f = 1{\cdot}0$, $\gamma_1 = 0{\cdot}4$, $\gamma_2 = 0{\cdot}6$. — —, $\theta = 0^\circ$; ——, 60°; – – –, 120°; —●—, 180°.

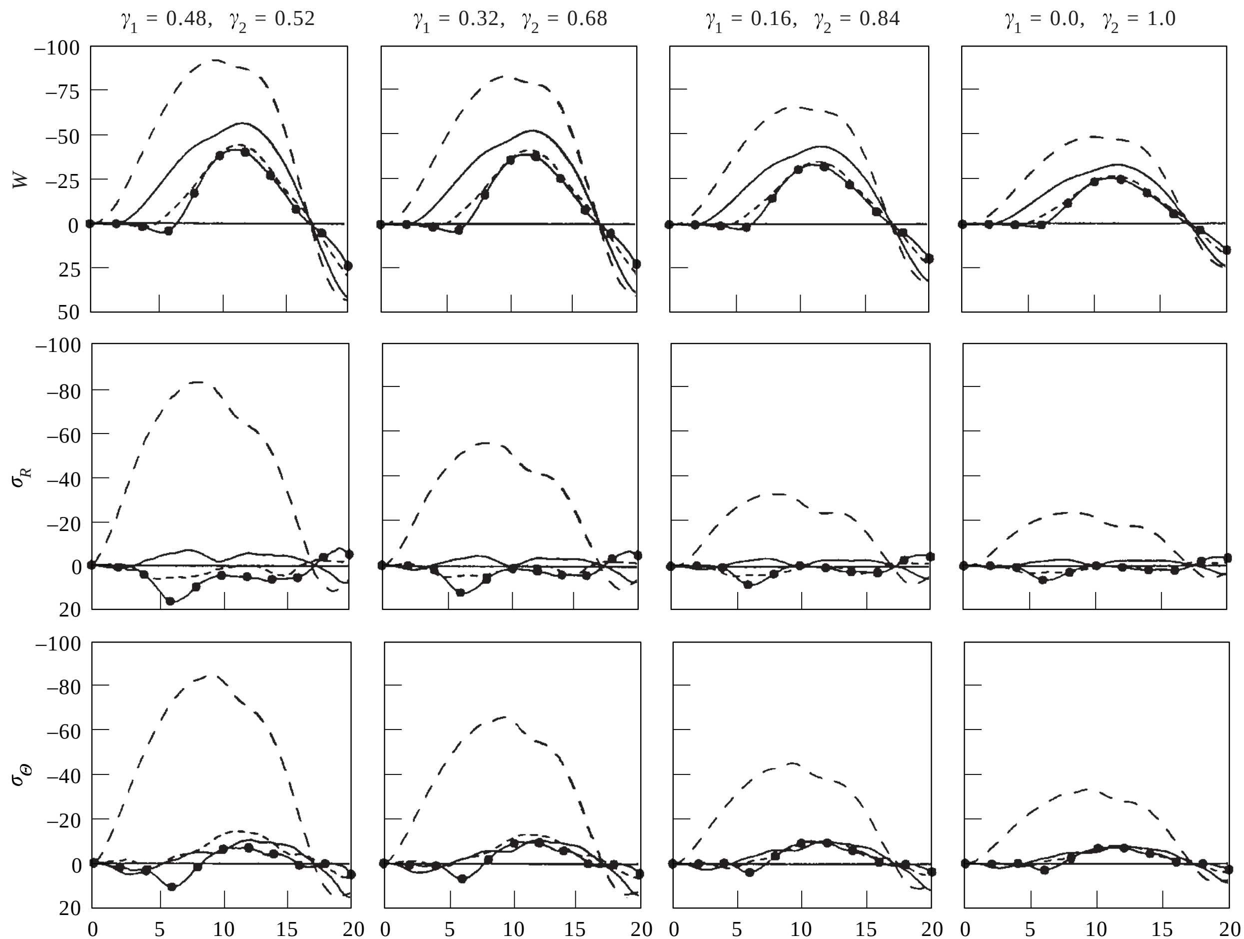

Figure 5. W, σ_R and σ_Θ at $R = 0{\cdot}5$ for plates subjected to pulse load for increasing radial span of load. $H_0 = 0{\cdot}01$, $\beta = 0{\cdot}3$, $R_f = 1{\cdot}0$, $\alpha = 2^\circ$. — —, $\theta = 0^\circ$; ——, 60°; – – –, 120°; —●—, 180°.

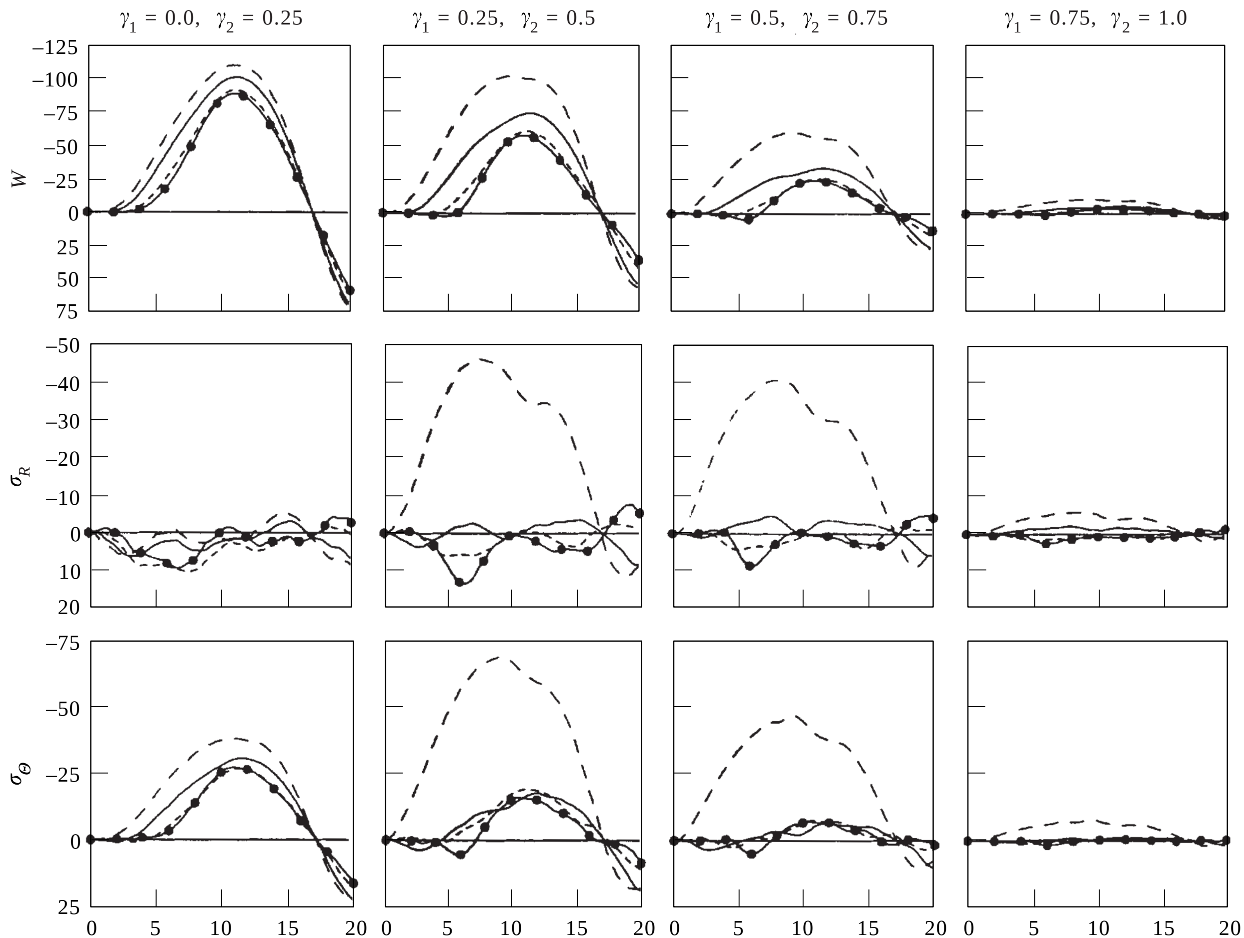

Figure 6. W, σ_R and σ_Θ at $R = 0{\cdot}5$ for plates subjected to pulse load for changing position of radial span of load. $H_0 = 0{\cdot}01$, $\beta = 0{\cdot}3$, $R_f = 1{\cdot}0$, $\alpha = 20^\circ$. — —, $\theta = 0^\circ$; ——, 60°; – – –, 120°; —●—, 180°.

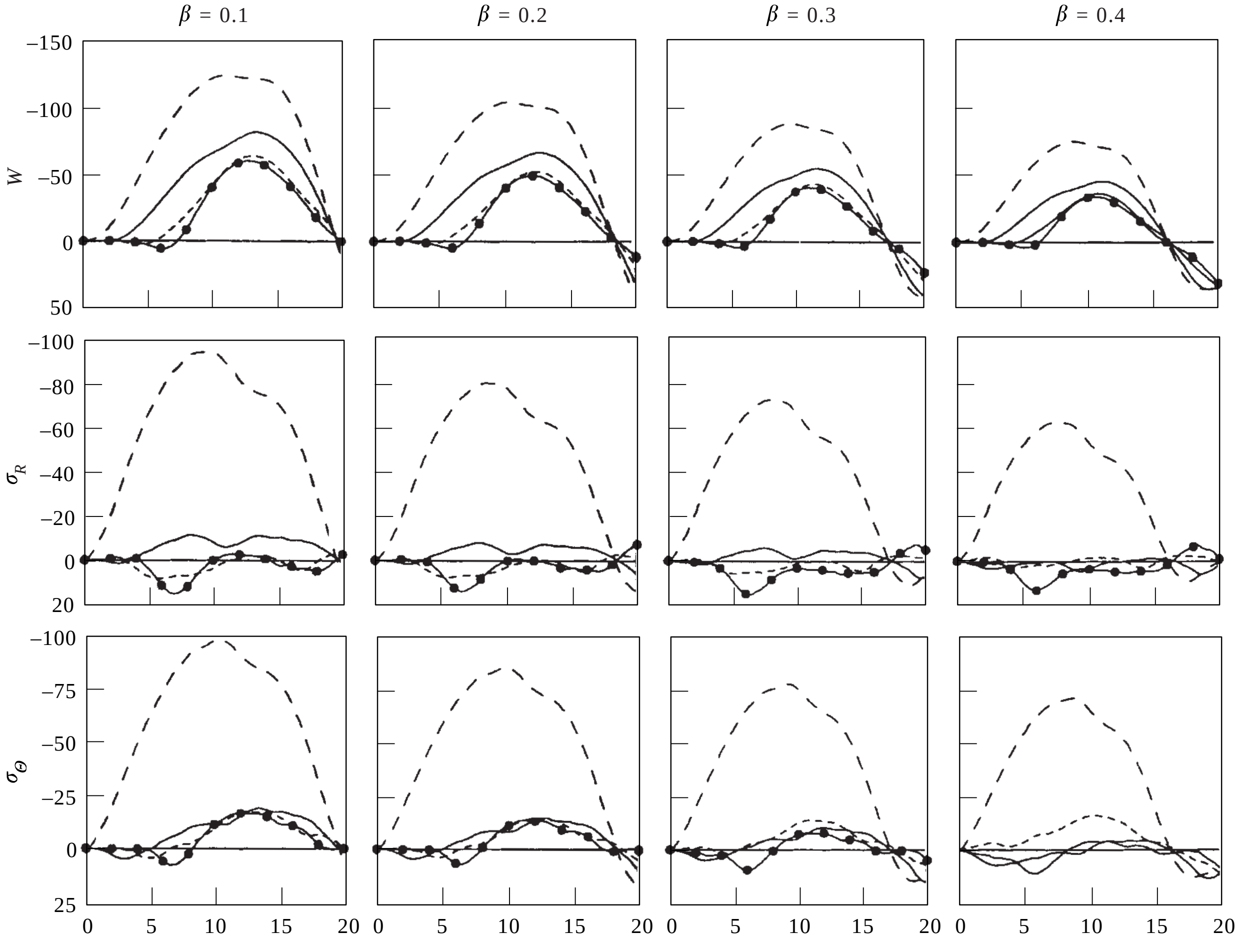

Figure 7. W, σ_R and σ_Θ at $R = 0{\cdot}5$ for plates subjected to pulse load for various values of β. $H_0 = 0{\cdot}01$, $R_f = 1{\cdot}0$, $\alpha = 20^\circ$, $\gamma_1 = 0{\cdot}4$, $\gamma_2 = 0{\cdot}6$. — —, $\theta = 0^\circ$; ——, 60°; – – –, 120°; —●—, 180°.

The variations in position, radial and angular span of the load are made in such a manner so that the total load on the plate remains constant.

Ramakrishnan and Kunukkasseril [13] presented results for transverse deflection, radial and tangential strains for a plate of constant thickness subjected to an off-center half-sine pulse point load for various pulse durations which were incorrect, as pointed out by Fisher [16]. The corresponding corrected results, obtained as a particular case, for a plate of constant thickness ($\beta = 0$) are presented in Figure 2. The results for transverse deflection match exactly those of Fisher [16].

W, σ_R, and σ_Θ at $R = 0{\cdot}5$ are plotted against time in Figures 3–7 for plates subjected to half-sine pulse load for various loading and plate parameters.

The effect of pulse duration on half-sine pulse load on the transverse deflection is illustrated in Figure 3. It can be seen that for short pulse durations, the time taken in attaining peak value of deflection is maximum for $\theta = 180^\circ$ and is maximum for $\theta = 0^\circ$. Also the deflection for $\theta = 180^\circ$ is more than the deflection along $\theta = 0^\circ$. But as the pulse duration increases, the time taken in attaining the peaks increases and is almost the same for all values of θ for $R_f \geqslant 1{\cdot}7$. At the same time, the deflection at $\theta = 0^\circ$ becomes maximum, whereas it becomes minimum at $\theta = 180^\circ$ and remains so for further increases in pulse duration. The increase in pulse duration continuously increases the time taken in attaining the peak values but the peak values are almost constant for $R_f \geqslant 3{\cdot}0$.

As the angular (α) and radial span ($\gamma_1 - \gamma_2$) of the load is increased, the asymmetry in W, σ_R, and σ_Θ is found to decrease, as is evident from Figures 4 and 5. This decrease in asymmetry is accompanied by a decrease in magnitude also. That is, if the loaded area increases, the asymmetry and the magnitude decrease.

If the position of the load is shifted from near the center of the plate towards its outer periphery, the asymmetry in transverse deflection and stresses first increases, becomes maximum for $\gamma_1 = 0{\cdot}25$ and $\gamma_2 = 0{\cdot}5$ and then decreases as is clear from Figure 6.

The effect of asymmetry in transverse deflection and stresses is more pronounced in thinner plates, as is evident from Figure 7 in which they are plotted for various values of the taper constant β.

REFERENCES

1. P. A. A. Laura, R. H. Gutierrez, R. Carnicer and H. C. Sanzi 1991 *Journal of Sound and Vibration* **144**, 149–161. Free vibration of a solid circular plate of linearly varying thickness and attached to a Winkler foundation.
2. V. Soamidas and N. Ganesan 1991 *Journal of Sound and Vibration* **147**, 39–56. Vibration analysis of thick, polar orthotropic variable thickness annular disks.
3. U. S. Gupta, R. Lal and S. K. Jain 1991 *Journal of Sound and Vibration* **147**, 423–434. Buckling and vibrations of polar orthotropic circular plates of linearly varying thickness and resting on elastic foundation.
4. J. S. Yang 1993 *Journal of Sound and Vibration* **165**, 178–184. The vibration of a circular plate with varying thickness.

5. P. A. A. Laura, C. Filipich and R. D. Santos 1977 *Journal of Sound and Vibration* **52**, 243–251. Static and dynamic behavior of circular plates of variable thickness elastically restrained along the edges.
6. T. Irie, G. Yamada and S. Aomura 1980 *International Journal of Mechanical Science* **22**, 99–107. The steady state response of a Mindlin annular plate of varying thickness.
7. B. V. de Greco and P. A. A. Laura 1984 *Journal of Sound and Vibration* **94**, 525–530. A note on the forced vibrations of a circular plate with thickness varying in a bilinear fashion.
8. A. P. Gupta and N. Goyal 1994 *International Journal of Mechanical Sciences* **36**, 439–448. Forced axisymmetric response of linearly tapered circular plates.
9. A. P. Gupta and N. Goyal 1995 *International Journal of Mechanical Sciences* **37**, 615–627. Effect of transverse shear and rotary inertia on the forced axisymmetric response of linearly tapered circular plates.
10. H. Reismann 1959 *Journal of Applied Mechanics* **26**, 526–527. Forced vibrations of a circular plate.
11. A. J. Mcleod and R. E. D. Bishop 1965 *Mechanical Engineering Science*. The forced vibration of circular flat plates. Monograph No. 1.
12. G. Anderson 1969 *Journal of Sound and Vibration* **9**, 126–144. On the determination of finite integral transform for forced vibrations of circular plates.
13. R. Ramakrishnan and V. X. Kunukkasseril 1974 *Journal of Sound and Vibration* **34**, 489–503. Asymmetric response of circular plates.
14. V. X. Kunukkasseril and R. Ramakrishnan 1974 *Journal of Sound and Vibration* **35**, 429–440. Sonic boom effects on circular bridge panels.
15. V. X. Kunukkasseril and K. Chandrasekaran 1975 *Experimental Mechanics* **15**, 424–428. Concentrated impact loading of circular plates.
16. H. D. Fisher 1979 *AIAA Journal* **17**, 1274–1276. Modal analysis of the transient asymmetric response of thin circular plates.
17. H. Q. Yang 1991 *AIAA Journal* **29**, 1529–1531. Generalized Kelvin function solution for a class of vibrating circular plate problems.